

Dilepton Measurements at STAR

Frank Geurts (for the STAR Collaboration)

Rice University, Houston, TX 77005, USA

E-mail: geurts@rice.edu

Abstract. In the study of hot and dense nuclear matter, created in relativistic heavy-ion collisions, dilepton measurements play an essential role. Leptons, when compared to hadrons, have only little interaction with the strongly interacting system. Thus, dileptons provide ideal penetrating probes that allow the study of such a system throughout its space-time evolution. In the low mass range ($M_{ll} < 1.1 \text{ GeV}/c^2$), the dominant source of dileptons originates from the decay of vector mesons which may see effects from chiral symmetry restoration. In the intermediate mass range ($1.1 < M_{ll} < 3.0 \text{ GeV}/c^2$), the main contributions to the mass spectrum are expected to originate from the thermal radiation of a quark-gluon plasma as well as the decays of charm mesons. In the high mass range ($M_{ll} > 3.0 \text{ GeV}/c^2$), dilepton measurements are expected to see contributions from primordial processes involving heavy quarks, and Drell-Yan production.

With the introduction of the Time-of-Flight detector, the STAR detector has been able to perform large acceptance, high purity electron identification. In this contribution, we will present STAR's recent dielectron measurements in the low and intermediate mass range for RHIC beam energies ranging between 19.6 and 200 GeV. Compared to electrons, muon measurements have the advantage of reduced bremsstrahlung radiation in the surrounding detector materials. With the upcoming detector upgrades, specifically the muon detector (MTD), STAR will be able to include such measurements in its (di-)lepton studies. We will discuss the future dilepton program at STAR and the physics cases for these upgrades.

1. Introduction

Dileptons have long been proposed as one of the more crucial probes in the study of the hot and dense matter [1]. Leptons do not experience the strong force, and thus will have negligible final state interactions in a strongly interacting medium, with a mean free path that is much larger than the typical size of this medium. Electromagnetic probes such as the dielectrons are emitted throughout the evolution of a heavy-ion collision. A typical dielectron invariant mass spectrum, therefore, involves a plethora of sources, ranging from Dalitz decays, which dominate the low invariant mass range, to Drell-Yan pair production which dominates at masses above $3 \text{ GeV}/c^2$. In addition, dilepton contributions originate from vector mesons, open heavy-flavor decays, and thermal radiation emitted from a quark-gluon plasma (QGP).

The subsequent stages in the evolution of a hot and dense nuclear system can be identified with certain ranges in the dilepton invariant mass spectrum. In the high invariant mass range ($M_{ll} > 3 \text{ GeV}/c^2$), dileptons from the decay of the heavy quarkonia such as the J/ψ and Υ mesons provide a means to study deconfinement effects in the hot and dense medium. These contributions are on top of a continuum from primordial Drell-Yan pair production. In the intermediate mass range ($1.1 < M_{ll} < 3.0 \text{ GeV}/c^2$), the production of dileptons is closely related to the thermal radiation of the QGP. However, at higher center-of-mass energies this signal

competes with significant contributions from open heavy-flavor decays such as $c\bar{c} \rightarrow e^+e^-X$, where such charm contributions may get modified by the medium. The prominent sources of dileptons in the low mass range ($M_{ll} < 1.1 \text{ GeV}/c^2$), in addition to the Dalitz decays, are the direct leptonic decays of the $\rho(770)$, $\omega(782)$, and $\phi(1020)$ vector mesons. The in-medium modification of the spectral shape of these mesons may serve as signature of chiral symmetry restoration. The ρ meson is of special interest given that in thermal equilibrium its contribution to the low mass range is expected to dominate through its strong coupling to the $\pi\pi$ channel [2]. Moreover, its short lifetime of $\tau \sim 1.3 \text{ fm}/c$, will make the spectral shape of this meson especially sensitive to in-medium modifications [3].

At SPS energies, the observed low-mass dilepton enhancement observed in both the CERES dielectron [3, 4] and NA60 dimuon data [5] could be explained in terms of in-medium effects on the spectral shape of the ρ meson. Moreover, the dimuon measurements by NA60 are found to favor significant broadening of the line shape over a mass-dropping model. At top RHIC energies, the PHENIX collaboration measured a significant enhancement in its dielectron measurements, with a strong p_T and centrality dependence [6]. However, models that have been able to describe the measurements at SPS energies are unable to consistently describe the PHENIX results in the most central collisions. The intermediate invariant mass range, between the ϕ and J/ψ mesons, opens an important window to thermal radiation from the QGP. However, contributions from the earlier mentioned semileptonic decays of open heavy-flavor hadrons are significant and need to be accounted for.

Direct photon measurements by the PHENIX collaboration in the range of $1 < p_T < 4 \text{ GeV}/c$ yielded a substantial elliptic flow, v_2 , comparable to the v_2 of hadrons [7]. Model calculations which include a dominant QGP thermal emission source significantly underpredicted the observed v_2 . However, incorporating a more detailed evolution of the hadronic phase, which involves the hadronic flow fields at chemical and kinetic freeze-out, appeared to improve the description of the direct photon v_2 reasonably well, while setting further constraints on the initial QGP temperatures [8]. Dilepton elliptic flow measurements as a function of p_T have been proposed as an independent measure to study the medium properties [9]. The combination of certain invariant mass and transverse momentum ranges allows for different observational windows on specific stages of the expansion. Dileptons can be used to further probe the early stages after a collision and possibly constrain the QGP equation of state.

The installation of the Time-of-Flight (TOF) detector [10] and the upgrade of its data acquisition (DAQ) system [11], allowed the STAR experiment to extend its large-acceptance particle identification capabilities and increase its DAQ rate. The TOF detector not only extends the reach of hadron identification to higher momenta, but also significantly improves the electron identification capability in the low momentum range. This, combined with the RHIC Beam Energy Scan (BES) program in 2010 and 2011, has put STAR in a unique position to measure dielectron spectra in the low and intermediate mass ranges from top RHIC beam energies down to SPS center-of-mass energies. In this paper, the preliminary dielectron results from the STAR experiment at top RHIC energy, $\sqrt{s_{NN}} = 200 \text{ GeV}$, are discussed as well as the preliminary results at several BES energies. The low invariant mass measurements are compared with recent model calculations. This paper concludes with an outlook on the future of the STAR dilepton program.

2. Electron Identification and Background Reconstruction

The electron identification for the results reported in the next sections involves the STAR Time Projection Chamber (TPC) and the TOF detector. The TPC detector is the central tracking device of the STAR experiment and it provides charged particle tracking and momentum measurement. The energy-loss measurements, dE/dx , in the TPC are used for particle identification. The TOF detector, with full azimuthal coverage at mid-rapidity, extends

the particle identification range to higher momenta. The combination of the TOF velocity information and the TPC energy loss allows for the removal of slower hadrons which contaminate the electron sample. The selection criteria for electron identification have been optimized for each RHIC beam energy. With an additional track momentum threshold of $p_T > 0.2$ GeV/ c , the electron purity in the minimum bias Au+Au analysis is 95%.

The unlike-sign invariant mass distributions, which are reconstructed by combining electrons and positrons from the same event, contain both signal and background contributions. Especially in high-multiplicity events, the contribution of the combinatorial background is large, see Fig. 1, and two methods have been used to estimate the background.

The mixed-event method combines electrons and positrons from different events with similar total particle multiplicity, vertex position along the beam line, and event-plane angle. While the statistical accuracy of the background description can be arbitrarily improved by involving more events, the mixed-event method fails to reconstruct correlated background sources. At the lower invariant masses, such correlated pairs arise from jets, double Dalitz decays, Dalitz decays followed by a conversion of the decay photon, or two-photon decays followed by the conversion of both photons [12]. A background estimation based on the like-sign method can account for such correlated contributions. Its drawback, however, is that the statistical accuracy is only comparable to the unlike-sign, *i.e.* the original raw mass spectrum. Moreover, the like-sign method will need to consider detector acceptance differences, in contrast to the (unlike-sign) mixed-event method.

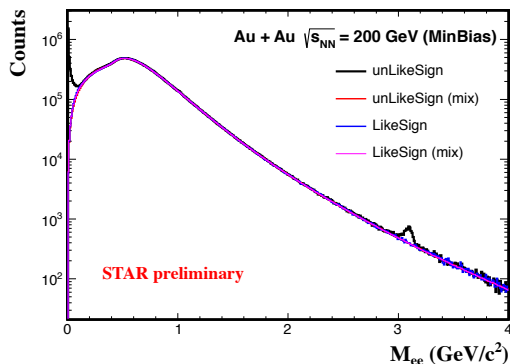


Figure 1. (Color online) Unlike-sign, like-sign, and mixed-event dielectron invariant mass distributions in Au+Au minimum bias collisions at $\sqrt{s_{NN}} = 200$ GeV.

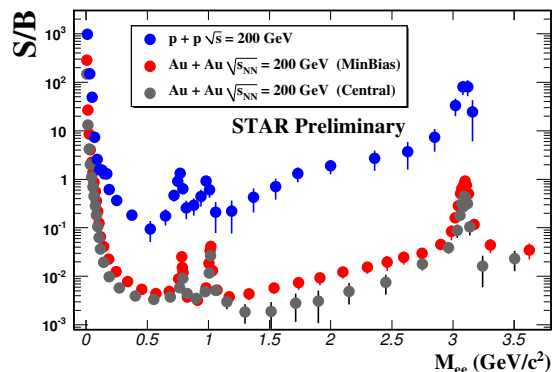


Figure 2. (Color online) Signal-to-background ratios in p+p, and Au+Au central, minimum bias events at $\sqrt{s_{NN}} = 200$ GeV [13].

The like-sign method is applied throughout the full mass range in Au+Au at $\sqrt{s_{NN}} = 19.6$ GeV, in the low mass range for $M_{ee} < 750$ MeV/ c^2 at $\sqrt{s_{NN}} = 200$ GeV, and for $M_{ee} < 900$ MeV/ c^2 at 39 GeV and 62.4 GeV. Above these respective invariant mass thresholds, the mixed-event method is applied [13, 14]. The signal-to-background ratios for 200 GeV p+p and Au+Au are shown in Fig. 2.

3. Dielectron Measurements at $\sqrt{s_{NN}} = 200$ GeV

The STAR experiment has recently published its results on dielectron measurements in p+p at $\sqrt{s} = 200$ GeV [15]. These results were based on 107 million p+p events taken in the 2009 RHIC run, with only a partially installed TOF system. The agreement between the measured

yields and the expected yields from a range of hadronic decays, heavy-flavor decays, and Drell-Yan production, provided an important verification of the analysis methods. More recently, the STAR experiment significantly improved its p+p data sample by about 700 million events with a fully installed TOF, effectively doubling its dielectron acceptance.

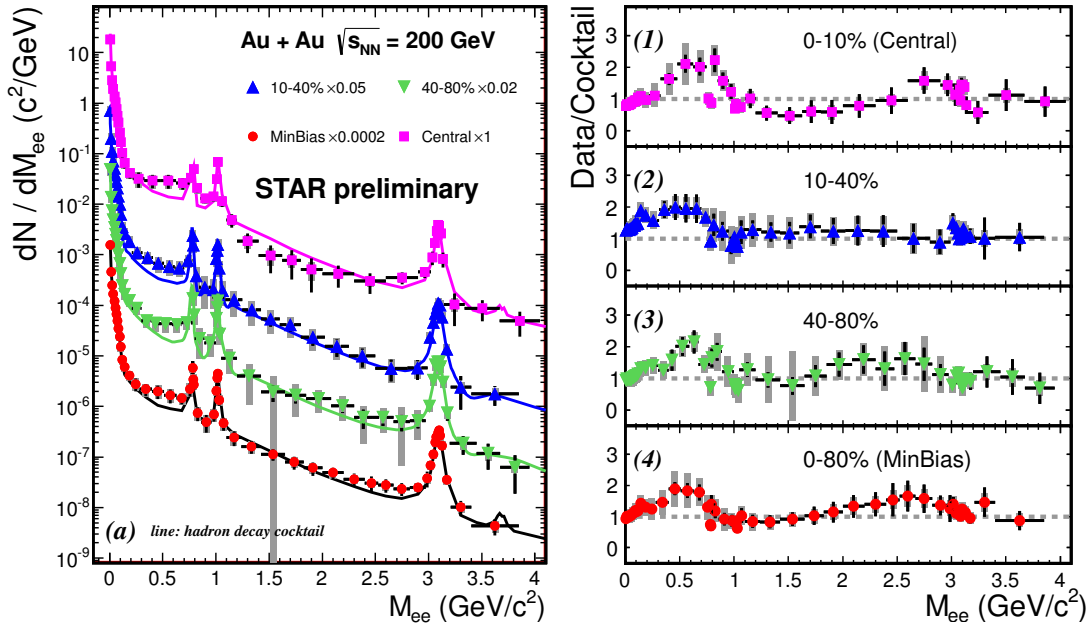


Figure 3. (Color online) Dielectron invariant mass spectra for Au+Au collisions at $\sqrt{s_{\text{NN}}}=200$ GeV for different centrality selections (left panel) and the ratio of data to cocktail (right panel). The systematical uncertainties are indicated by boxes.

The left panel of Fig. 3 presents for Au+Au collisions at $\sqrt{s_{\text{NN}}}=200$ GeV the centrality dependence of the invariant mass spectra in the STAR acceptance ($|y_{ee}| < 1.0$, $|\eta_e| < 1$, and $p_{\text{T}} > 0.2$ GeV/c). The measured yields are compared to a cocktail simulation of expected yields where the hadronic decays include the leptonic decay channels of the ω , ϕ , and J/ψ vector mesons, as well as the Dalitz decays of the π^0 , η , η' mesons [13]. The input distributions to the simulations are based on Tsallis Blast-Wave function fits to the invariant yields of the measured mesons [12]. These functions serve as the input distributions for the GEANT detector simulation using the full STAR detector geometry. The ρ meson contributions have not been included in the cocktails as it may be sensitive to in-medium modifications which are expected to affect this meson's spectral line shape [16]. In the intermediate mass range, the $c\bar{c}$ cross section is based on PYTHIA simulations scaled by the number of nucleon-nucleon collisions [17]. The cocktail simulations are observed to overestimate the data in central collisions. This can indicate a modification of the charm contribution. However, the observed discrepancy is still consistent within the experimental uncertainties.

In the right panels of Fig. 3, the ratios of the data to cocktail yields have been depicted for different centrality selections. A clear enhancement in the low mass range can be observed. As the charm contributions scale with the number of binary collisions, the total cocktail yield increases with centrality, and only little centrality dependence can be observed in the ratio plots. On the other hand, as can be seen in Fig. 4, a comparison of the dilepton yield dN/dM_{ee} in the range of $150 < M_{ee} < 750$ MeV/ c^2 scaled to the number of participants, N_{part} , appears to indicate an increase of the low-mass-range enhancement with increasing centrality. Such an

increase, albeit with large uncertainties, would agree with similar observations reported in [4].

Figure 5 shows the inclusive dielectron transverse mass slopes, in the intermediate mass range, measured in p+p and Au+Au at $\sqrt{s_{NN}}=200$ GeV. The m_T slopes in this plot have been determined for $1.1 < M_{ee} < 1.8$, $1.8 < M_{ee} < 2.8$ GeV/ c^2 in Au+Au and $1.1 < M_{ee} < 1.6$, $1.6 < M_{ee} < 2.9$ GeV/ c^2 , respectively. These measurements are compared with the slope parameters of hadrons (circles) and charm/Drell-Yan subtracted dimuon measurements (open squares, [18]). While the p+p results (triangles) are consistent with PYTHIA calculations, the transverse mass slopes in Au+Au collisions (filled squares) are observed to be larger than those in p+p. This is indicative of a possible combination of both thermal dilepton production and charm modification. Future detector upgrades will allow STAR to further disentangle the potentially modified charm contributions and help provide improved measurements of the thermal QGP dilepton radiation.

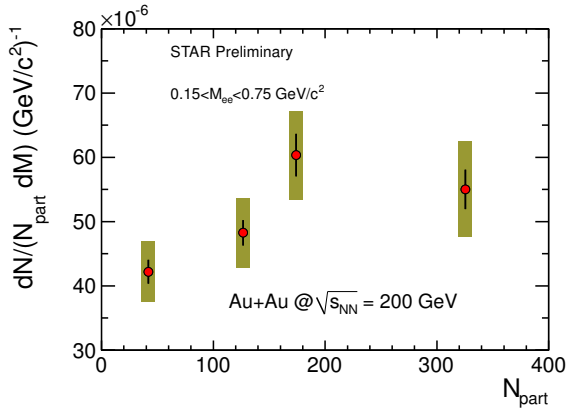


Figure 4. (Color online) Dielectron LMR yields scaled by N_{part} versus centrality (N_{part}) for Au+Au collisions at $\sqrt{s_{NN}}=200$ GeV [19]. The boxes indicate the systematical uncertainty.

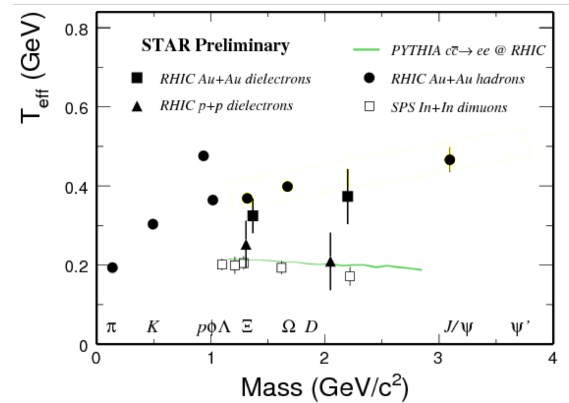


Figure 5. Transverse mass slope parameters from Au+Au at $\sqrt{s_{NN}}=200$ GeV (RHIC) and In+In at $\sqrt{s_{NN}}=17.2$ GeV (SPS) energies [13].

The STAR dielectron elliptic-flow measurements in Au+Au at $\sqrt{s_{NN}} = 200$ GeV as a function of the dielectron invariant mass are presented in Fig. 6. These preliminary results are based on 700 million minimum bias events involving an analysis that combined the data sets from the 2010 and 2011 RHIC Runs. The elliptic flow, v_2 , is calculated using the event-plane method in which the event plane has been reconstructed from TPC tracks [20]. The “signal” elliptic flow, v_2^{signal} , is calculated as follows [21]:

$$v_2^{\text{total}}(M_{ee}) = v_2^{\text{signal}}(M_{ee}) \frac{r(M_{ee})}{1 + r(M_{ee})} + v_2^{\text{bkgd}}(M_{ee}) \frac{1}{1 + r(M_{ee})},$$

where v_2^{total} is the flow measurement of all dielectron candidates, v_2^{bkgd} the flow measurement of the dielectron background, and $r(M_{ee})$ the mass-dependent signal-to-background ratio. The expected v_2 from a cocktail simulation based on the contributions from π^0 , η , ω , and ϕ mesons is within uncertainties consistent with the measurements.

Differential measurements have been done as a function of centrality (not shown here) and p_T , as shown in Fig. 7. Both $v_2(p_T)$ for different dielectron mass windows, and its centrality dependence in the lower mass bin show a consistency between the measurements and the simulations. Work is underway to further extend these measurements into the intermediate

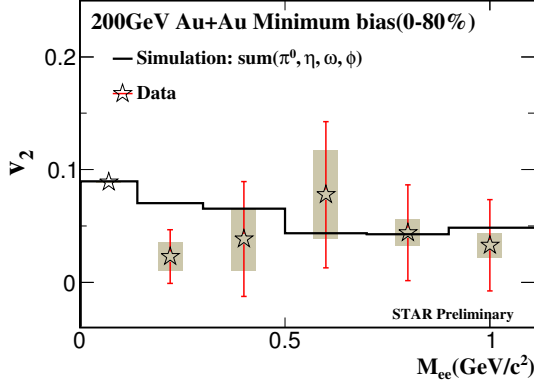


Figure 6. (Color online) Dielectron elliptic flow as a function of the invariant mass in minimum-bias Au+Au collisions at $\sqrt{s_{NN}} = 200$ GeV. The boxes indicate the systematic uncertainty. The black line is the sum of a simulation which involved π^0 , η , ω , and ϕ -mesons.

mass range. However, it will be important to disentangle the charm contributions at higher M_{ee} . The current experimental uncertainties on the STAR data points are still too large to allow for further constraints on the QGP equation of state, as is conjectured in *e.g.* [9].

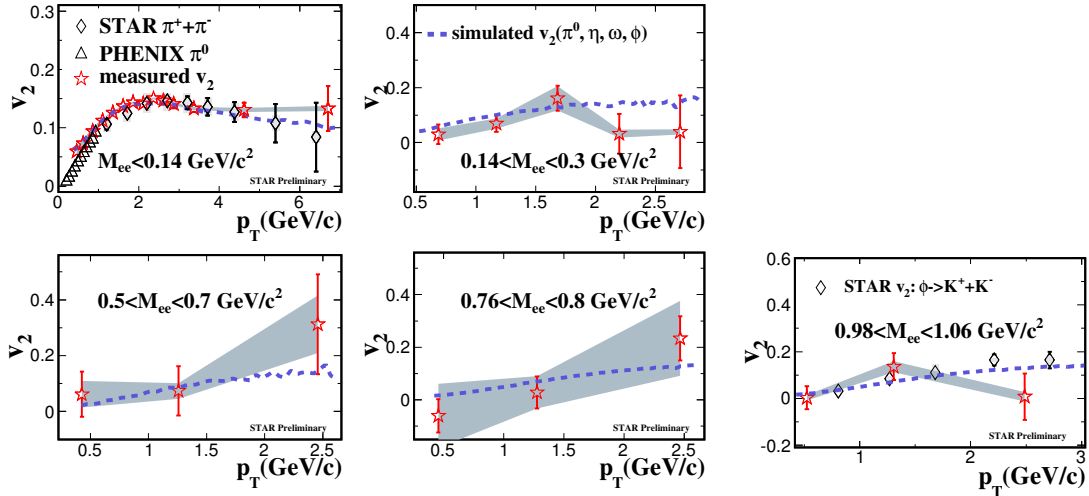


Figure 7. (Color online) Elliptic flow, v_2 , as a function of p_T for various dielectron invariant mass ranges in minimum-bias collision Au+Au collisions at $\sqrt{s_{NN}} = 200$ GeV (red stars). In addition, in the upper left panel the v_2 of π^0 [22] and π^\pm mesons [23] are shown. The ϕ meson v_2 measurements in the lower right panel are from STAR. The blue dashed lines are the expected v_2 from cocktail simulations (see text). The grey bands indicate the systematic uncertainties.

4. Dielectron Measurements in the Beam Energy Scan Program

Measurements performed at top RHIC energies by both the STAR and PHENIX [6] collaborations indicate a significant enhancement in the low mass range when compared to a hadron cocktail simulation of the expected yields. Such an enhancement may point to in-medium modification effects that possibly result from chiral symmetry restoration. At the SPS,

measurements performed by the NA60 [5] and CERES [3, 4] collaborations also show a low-mass enhancement which favors a broadening of the ρ meson spectral shape when compared to a dropping-mass scenario. The Beam Energy Scan (BES) program at RHIC allowed the STAR collaboration to systematically explore the dielectron production from $\sqrt{s_{NN}} = 200$ GeV down to SPS beam energies.

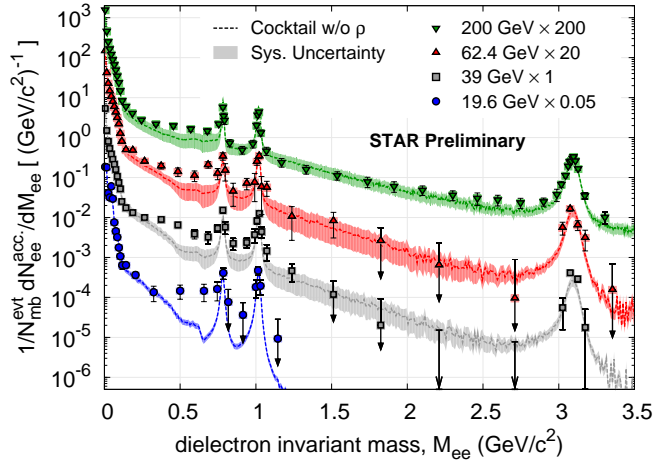


Figure 8. (Color online) Background-subtracted dielectron invariant-mass distributions from Au+Au collisions at $\sqrt{s_{NN}} = 19.6, 39, 62.4,$ and 200 GeV. The (colored) dotted lines show the hadron cocktails (excluding contributions from ρ mesons). The (color) shaded areas indicate the systematic uncertainties.

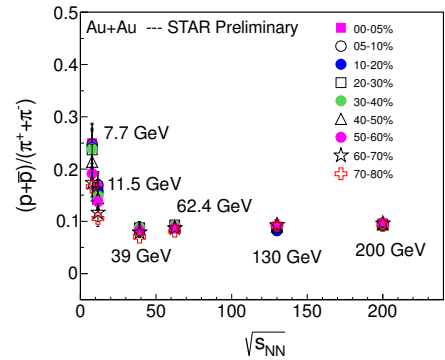


Figure 9. (Color online) $(p+\bar{p})/(\pi^++\pi^-)$ in Au+Au collisions as a function of the center-of-mass energy $\sqrt{s_{NN}}$.

In Fig. 8, the inclusive invariant mass spectra in Au+Au collisions for $\sqrt{s_{NN}} = 19.6, 39, 62.4,$ and 200 GeV are shown, together with the hadron cocktail simulations for each energy. The cocktail simulations exclude contributions from the ρ meson. For each of the energies a significant enhancement in the low mass range can be observed. While a quantitative discrepancy remains between the PHENIX and STAR measurements at $\sqrt{s_{NN}} = 200$ GeV [6, 24], the preliminary STAR results are comparable with the CERES measurements in the Pb+Au system at $\sqrt{s_{NN}} = 17.2$ GeV albeit with differences in acceptance [3, 14]. Moreover, various models have shown good agreement with the low-mass spectrum measured by STAR in central Au+Au collisions at $\sqrt{s_{NN}} = 200$ GeV [25, 26, 27]. The in-medium broadening of the ρ meson is expected to be driven by the strong coupling to baryons and thus the total baryon density since the vector mesons interact symmetrically with baryons and antibaryons [3, 27]. At SPS beam energies with substantial nuclear stopping, most baryons are participating nucleons. At RHIC top energies nuclear stopping and thus the net-baryon density will vanish and a significant baryon-antibaryon production is expected to compensate the total baryon density. As shown in Fig. 9, the total baryon density at freeze-out as a function of $\sqrt{s_{NN}}$ does not change significantly with center-of-mass energies down to 20 GeV. Accordingly, models that show good agreement at SPS and top-RHIC energies should be able to describe the low-mass enhancement throughout the BES center-of-mass energies.

In Fig. 10, the efficiency-corrected invariant mass spectra are shown for minimum bias Au+Au collisions at $\sqrt{s_{NN}} = 19.6, 62.4,$ and 200 GeV, respectively. In each of the three panels the hadron cocktail simulations include contributions from Dalitz decays, photon conversions (19.6 GeV only), and the dielectron decay of the ω and ϕ vector mesons. As is the case for the previously described 200 GeV cocktail simulations, contributions from ρ mesons have been

excluded. Instead, the ρ meson is explicitly included in the model calculations by Rapp [2, 27] which involve in-medium modifications of the ρ meson spectral shape. In this model a complete evolution of the QGP and thermal dilepton rates in the QGP and hadron-gas (HG) phases are convoluted with an isentropic fireball evolution. In the HG phase the ρ “melts” when extrapolated close the conjectured phase transition boundary. Moreover, it has been noted that the top-down extrapolated QGP rates closely coincide with the bottom-up extrapolated hadronic rates [2]. The measured low-mass enhancement can consistently be described by these model

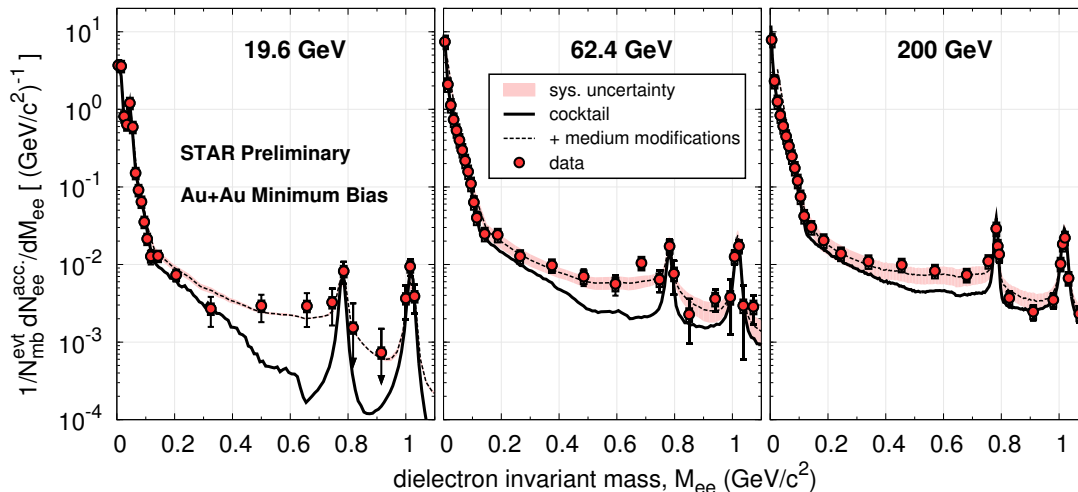


Figure 10. (Color online) BES dielectron invariant-mass distributions in the low invariant-mass range from Au+Au collisions at 19.6 GeV (left), 62.4 GeV (middle), and 200 GeV (right panel). The red data points include both statistical and systematic uncertainties (boxes). The black curve depicts the hadron cocktail, while the dashed line shows the sum of the cocktail and model calculations. The latter includes contributions from both the HG and the QGP phases. The systematic uncertainty on the former is shown by the light red band.

calculations and agrees with a scenario in which the in-medium modification of the ρ involves a broadening of its spectral function.

Differential studies of the low-mass dielectron distributions as a function of the center-of-mass energy, centrality, and p_T will allow for a more detailed comparison against these chiral hadronic models. Further comparisons between these models, lattice QCD calculations, and experimental data could help provide explicit evidence of chiral symmetry restoration in heavy-ion collisions.

5. Future Directions of the STAR Dilepton Program

Measuring dileptons is a challenging task where very small signals sit on top of large combinatorial and physics backgrounds. With the recent TOF upgrade, the STAR experiment is able to address some of the important physics questions that involve the low and intermediate dielectron mass ranges. In the low mass range, STAR’s measurements agree with results at SPS energies in which the enhancement is attributed to the broadening of the ρ meson. Moreover, model calculations by Rapp [27] appear to be able to describe the BES data at the intermediate center-of-mass energies. In the future, additional verification of the robustness of such a description will be allowed by the inclusion of independent analyses of other BES data sets. Differential measurements will further verify the consistency of such models and advance the study of chiral symmetry restoration.

As the typical production rates for dileptons are rather small, large event samples are needed to make significantly accurate measurements in both the low and intermediate mass ranges. Especially at the lower RHIC beam energies, the statistical uncertainties are very large (see Fig. 8). The $\sqrt{s_{NN}}=19.6$ GeV measurements are based on 28 million Au+Au collisions. To achieve statistical uncertainties at a level of 10% and improve the understanding of the baryonic component to the in-medium effects on the vector mesons, a factor of 10 more statistics would be required. For such an increase in total luminosity at RHIC, requires the development and installation of electron cooling components.

Cocktail simulations indicate that at top RHIC energies the correlated charm contributions dominate the intermediate-mass range dielectrons. The PYTHIA simulations that are used for the cocktail simulations assume no medium effects and have been rescaled to match the charm cross sections to, *e.g.*, 0.96 mb in 200 GeV Au+Au collisions. Both assumptions result in large uncertainties, with some hints that point to a suppression of the charm contribution in central collisions when compared to the minimum-bias data (see Fig. 3). These uncertainties directly affect the extraction of any intermediate-mass dilepton signals related to the thermal QGP radiation. With the dominant source of intermediate-mass $e - \mu$ correlations originating from the $c\bar{c}$ correlated pair decays, measuring this correlation will be an essential tool for isolating the QGP thermal contribution in the intermediate mass range. Upcoming STAR detector upgrades [28] will, among many other key measurements, significantly improve our understanding of the charm contribution at intermediate dilepton masses. The Muon Telescope Detector (MTD) will provide a dedicated trigger for and the measurement of these electron-muon correlations, where both leptons are measured at mid-rapidity.

With the primary focus of the MTD physics program [29] on the quarkonia measurements at RHIC energies, the large-acceptance muon detector will also allow the STAR dilepton physics program to include the dimuon measurements of QGP thermal radiation, light vector mesons, and Drell-Yan production. The MTD is expected to be fully commissioned in 2014.

Acknowledgments

This work is supported by the US Department of Energy under grant DE-FG02-10ER41666.

References

- [1] E. Shuryak, Phys. Lett. B78 (1978) 150.
- [2] R. Rapp, J. Wambach, H. van Hees, arXiv:0901.3289v1 [hep-ph].
- [3] D. Adamová *et al.*, Phys. Lett. B 666 (2008) 425.
- [4] G. Agakichiev *et al.*, Eur. Phys. J. C 41 (2005) 475.
- [5] R. Arnaldi *et al.*, Eur. Phys. J. 59 (2009) 607.
- [6] A. Adare *et al.*, Phys. Rev. C 81 (2010) 034911.
- [7] A. Adare *et al.*, arXiv:1105.4126.
- [8] H. van Hees, C. Gale, and R. Rapp, Phys. Rev. C 84 (2011) 054906.
- [9] R. Chatterjee *et al.*, Phys. Rev. C 75 (2007), 054909.
- [10] W. Llope (for the STAR Collaboration), Nucl. Instr. and Meth. A 661 (2012), S110.
- [11] J. Landgraf *et al.*, Nucl. Instr. and Meth. A 499 (2003), 762.
- [12] L. Ruan (for the STAR Collaboration), Nucl. Phys. A 855 (2011), 269.
- [13] J. Zhao (for the STAR Collaboration), J. Phys. G: Nucl. Part. Phys. 38 (2011), 124134.
- [14] B. Huang, proceedings QM 2012, accepted by Nucl. Phys. A.
- [15] L. Adamczyk *et al.*, Phys. Rev. C 86 (2012) 024906.
- [16] J. Adams *et al.*, Phys. Rev. Lett. 92 (2004), 092301.
- [17] J. Adams *et al.*, Phys. Rev. Lett. 94 (2005), 062301.
- [18] R. Arnaldi *et al.*, Phys. Rev. Lett. 100 (2008), 022302.
- [19] L. Ruan, *Rapporteur Talk: Heavy Flavor, Quarkonia and Electroweak Probes*, QuarkMatter 2012.
- [20] B. Adelev *et al.*, Phys. Rev. C 77 (2008), 054901.
- [21] B. Huang (for the STAR Collaboration), Acta Phys. Pol. B Proc. 5 (2012), 471.
- [22] S. Afanasiev *et al.*, Phys. Rev. C 80 (2009), 054907.

- [23] Y. Bai, Ph.D. Thesis, Universiteit Utrecht, The Netherlands (2007).
- [24] F. Geurts (for the STAR Collaboration), arXiv:1208.3437 [nucl-ex]
- [25] O. Linnyk *et al.*, Phys. Rev. C 85 (2012) 024910.
- [26] H. Xu *et al.*, Phys. Rev. C 85 (2012) 024906.
- [27] R. Rapp, Phys. Rev. C 63 (2001) 054907; R. Rapp, private communication.
- [28] F. Videbaek, these proceedings.
- [29] L. Ruan *et al.*, J. Phys. G: Nucl. Part. Phys. 36 (2009) 095001.